BeBeC-2012-01

Berlin Beamforming Conference 2012

LOCALISATION OF SOUND SOURCES ON AIRCRAFT IN FLIGHT

Henri A. Siller
German Aerospace Center (DLR)
Institute of Propulsion Technology, Engine Acoustics
henri.siller@dlr.de
Mueller-Breslau-Str. 8, 10623 Berlin, Germany

ABSTRACT

Sound sources on aircraft in flight can be localised and analysed using phased microphone arrays. The flight trajectory has to be known in order to reconstruct the signal at the source from the Doppler shifted microphone data and map the sound sources by applying time domain beamforming. Different array types can be used depending on the equipment available, other constraints of the experiment, and the desired spatial resolution and dynamic range of the sound source maps. In order to obtain quantitative results, a deconvolution of the maps with the point spread function of the array has to performed. This compensates the imaging properties of the microphone array. From the deconvoluted source maps, the acoustic power can be integrated over different source regions in order to obtain a ranking of the sources.

1 INTRODUCTION

Fly-over tests with microphone arrays are a valuable diagnostic tool for the localization and the analysis of aircraft noise sources. They are the only method to accurately measure the sound sources of an aircraft in flight, which cannot be fully represented in wind-tunnel or numerical simulations because they are either not known or difficult to resolve in model scale.

Among other groups, namely ONERA in France [21], NLR in the Netherlands [24], and the Boeing QTD progamme in the USA [28, 29], the Department of Engine Acoustics at the DLR Institute of Propulsion Research has developed and refined methods to localize and analyse the sound sources on aircraft in flight from array measurements. The method is based on the delay-and-sum beamforming algorithm [13], which saw its first application in the aircraft industry in an investigation of the jet noise of the Olympus engine of the Concorde [2]. At DLR, the beamforming method was extended to moving sources for the analysis of sound sources on

Figure 1: A Boeing 747 passing over a large microphone array set up by DLR for the fly-over measurements performed by DLR and Lufthansa in September 2008 at Parchim Airport

high-speed trains [1]. It was first applied to aircraft in flight in the 1990s [14] and DLR has constantly improved the method since. In the year 2001, DLR and Lufthansa started a cooperation in the framework of the research network *Leiser Verkehr*, which continues on today. In German national research projects (LAnAb, see [17] and FREQUENZ, see [5]), extensive array measurements of the A319, the MD-11, and the B747 aircraft were performed. In European research projects (e.g. C-Wake, Silence(r), and AWIATOR), DLR has performed array measurements of the A319 and A340 in cooperating with ONERA and Airbus. Array measurements were also performed under industrial contracts with Lufthansa, Airbus, and Embraer. Altogether, array data from fly-over measurements have been recorded for many different aircraft types, mainly for the Airbus models A319/20, A340, A380, the Boeing 747, the MD-11 and the Embraer 170 [6, 16, 18, 19, 23, 26, 27].

From the first experiments in the late 1990s with a linear microphone array with 24 microphones, the size of the microphone arrays and the number of microphones has been increased with the technical progress of digital data acquisition systems.

The source distributions calculated with the beamforming algorithm are the result of a convolution of the source distribution and the imaging properties of the array. The results are of a qualitative nature, but serve well to localize tonal sources and to analyse the frequency content and the directivity of the sources.

A quantitative analysis of phased array data for moving sources based on a deconvolution of the sound source maps with the point spread function of the microphone array has been developed at DLR since 2005[7, 8]. The deconvolution method improves the spatial resolution and the dynamic range of the source maps and allows a quantitative analysis of the source levels.

The state of the art method for source localization on aircraft in flight is to use large multi-arm spiral arrays with diameters of up to 35 meters and up to 240 microphones (see figure 2). Such a set-up can be used to map noise sources on an aircraft at fly-over altitudes of typically 200-600 feet. The array data is analysed using a classical beamforming algorithm in the time domain with a subsequent deconvolution of the sound source maps.

The deconvolution greatly improves the spatial resolution and the dynamic range of the source maps and yields quantitative results. The amplitudes of the sound sources can be integrated over different source regions on the aircraft. The results of the integration can be used to quantify the contribution of individual source regions to the total noise emitted by the aircraft and the sources can be listed in rank order. Using this information, noise abatement measures can be devised effectively in terms of costs and acoustic benefit.

2 EXPERIMENTAL SET-UP AND PROCEDURE

2.1 Considerations and constraints of fly-over measurements

Fly-over experiments with full-sized aircraft are expensive because of the cost of the aircraft itself and because a lot of time may have to be spent waiting for the right meteorological conditions. Acoustic fly-over tests should only be performed under the atmospheric conditions that are prescribed for noise certification in ICAO Annex 16 [10]. The acceptable temperate and humidity limits are defined in ISO3891 [11].

Acquiring a consistent and complete data set in an acoustic fly-over test is not easy, because the time for the measurements is restricted by the availability of the aircraft, by atmospheric conditions and daylight hours. Only a limited number of flights can be performed during each test day and it may not always possible to repeat invalid fly-overs. Therefore, a test matrix for a fly-over test has to be designed very carefully. A priority of configurations has to be fixed and extra time has to be allowed for repeat measurements.

In preparation of the fly-over test, the array has to be set up and ready to measure before the first fly-over. The microphone positions have to be known precisely, because the accuracy of the position determines the phase error between different microphones. The flight path of the aircraft has to be monitored and recorded together with a reference time signal that can later be used for synchronisation with the acoustic data. All the equipment used for the test has to be fit for prolonged outdoor use. It has to withstand the effects of rain, heat, and condensation in the morning and evening hours. The outdoor test conditions are very demanding especially on the microphones.

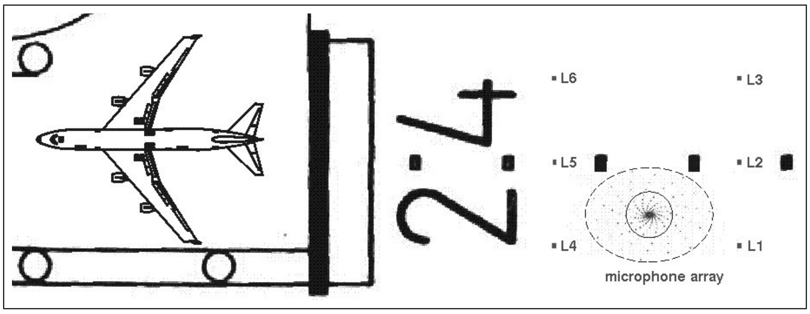

Figure 2: The set-up of the 43x36 m multi-arm spiral array for the B747 fly-over measurements of DLR and Lufthansa at Parchim airport, 2008; the aircraft on the runway is shown in order to indicate the relative size, the points L1–L6 mark the locations of the laser distance meters.

2.2 Design and layout of the microphone array

Almost any array shape can and has been used for fly-over tests, e.g. linear arrays [15], cross-shaped arrays [20], and complex geometries with multi-arm spirals or random arrangements (e.g. [6, 27]). Every array has different properties and may have its merits depending on the desired results, the available hardware and environmental constraints of the experiment.

A microphone array has to be designed according to the desired spatial resolution in the frequency range of interest for the given flight altitudes. The beam width of the array is proportional to the wavelength λ, the distance between the array and the aircraft r and inversely proportional to the diameter of the array d and the projection of the array in the direction of the aircraft:

$$b \approx \frac{\lambda\, r}{d \sin^3 \theta_e} \,. \tag{1}$$

The emission angle θ_e is the angle between the flight path and the direct line from the reference point on the aircraft to the array center point at emission time.

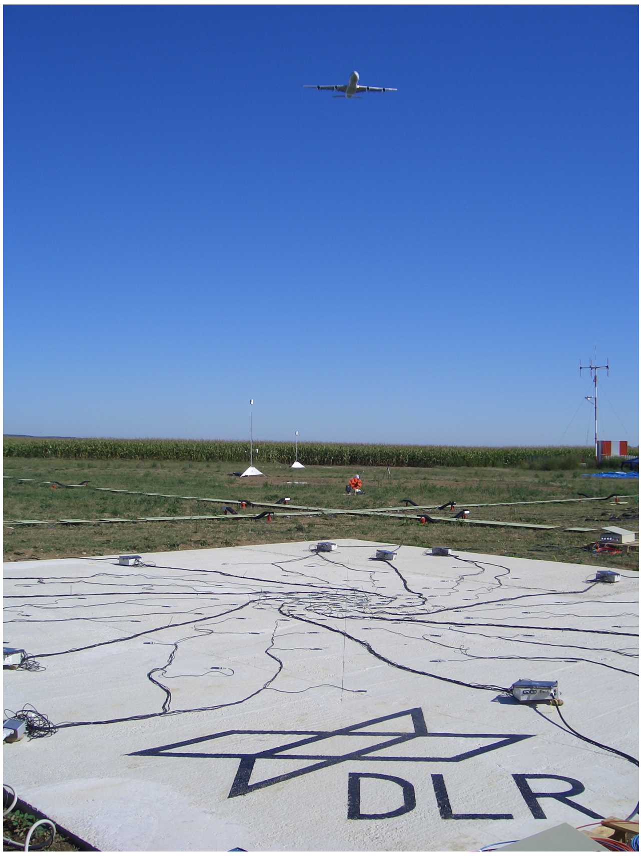

Figure 3: The spiral microphone array of DLR and the cross array of ONERA used in the EU project AWIATOR in 2006.

The way in which the microphones are arranged has an influence on the beamforming results. Today, mainly two general set-ups are used: arrays derived from a combination of linear microphone arrangements, like the cross or X-shaped array and more or less randomized planar distributions of microphones, like the multi-arm spiral arrays used by DLR. The cross-shaped array, which has been the set-up of choice of ONERA [19, 20] and Airbus for some time, gives good resolution with relatively few microphones at the expense of aliases at positions 45° from the main axes of the aircraft. The spiral array, which has no symmetries, yields better results at the expense of more work involved in the set-up and maintenance of the array during the test. Figure 3 shows a combination of both array types for the A340 fly-over tests in the EU project AWIATOR in 2006, where DLR had set up a multi-arm spiral array for the higher frequency range above 1250 Hz and ONERA a cross-shaped array for the low frequency range.

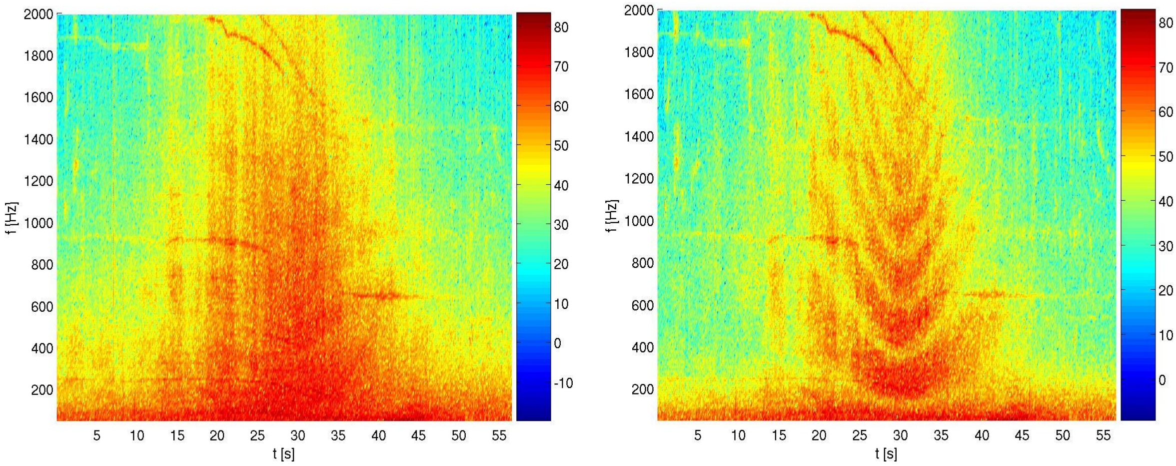

Figure 4: Spectrograms calculated from simultaneous recordings of one flyover with a ground microphone (left) and a microphone mounted $1.2\,m$ *above ground (right).*

2.3 Installation of the microphones

The way the microphones are mounted is a critical issue, because of changes in the directivity of the microphones at higher frequencies and possible refraction and wave superposition effects. The sensitivity of a cylindrical microphone is a function of the polar angle of the sound waves relative to the membrane of the microphone. The polar directivity of a cylindrical microphone is usually almost uniform for low frequencies, but deviates for high frequencies. This effect is usually negligible for the interesting frequency range below 10 kHz. The best solution to get close to uniform directivity is to mount microphones onto a large flat surface with the membrane parallel to the ground plane. A good compromise is to use cylindrical microphones placed flat on the ground at grazing incidence to the sound waves, i.e. with the microphone axis perpendicular to the direction of flight.

Apart from the directivity of the microphone itself, the position of the array relative to the ground and changes in the ground impedance around the microphone have an effect on the results. Ground microphones measure the direct sound only and the measured sound pressure level is 6 dB higher than in the free-field due to the pressure doubling at the ground.

If microphones are mounted at some distance above the ground, the direct and the reflected sound waves superimpose at the microphone and generate a frequency dependent pattern of constructive and destructive interference. Figure 4 presents results from simultaneous recordings of an aircraft fly-over with a pair of microphones, one on mounted on a ground plate, the other 1.2 m above ground. The data are presented as spectrograms, i.e. short-time Fourier transforms as a function of time The spectrogram of the 1.2 m microphone clearly shows the typical cancellation lobes: the interference of the direct and the reflected sound waves generates successive minima and maxima of the sound pressure at different frequencies.

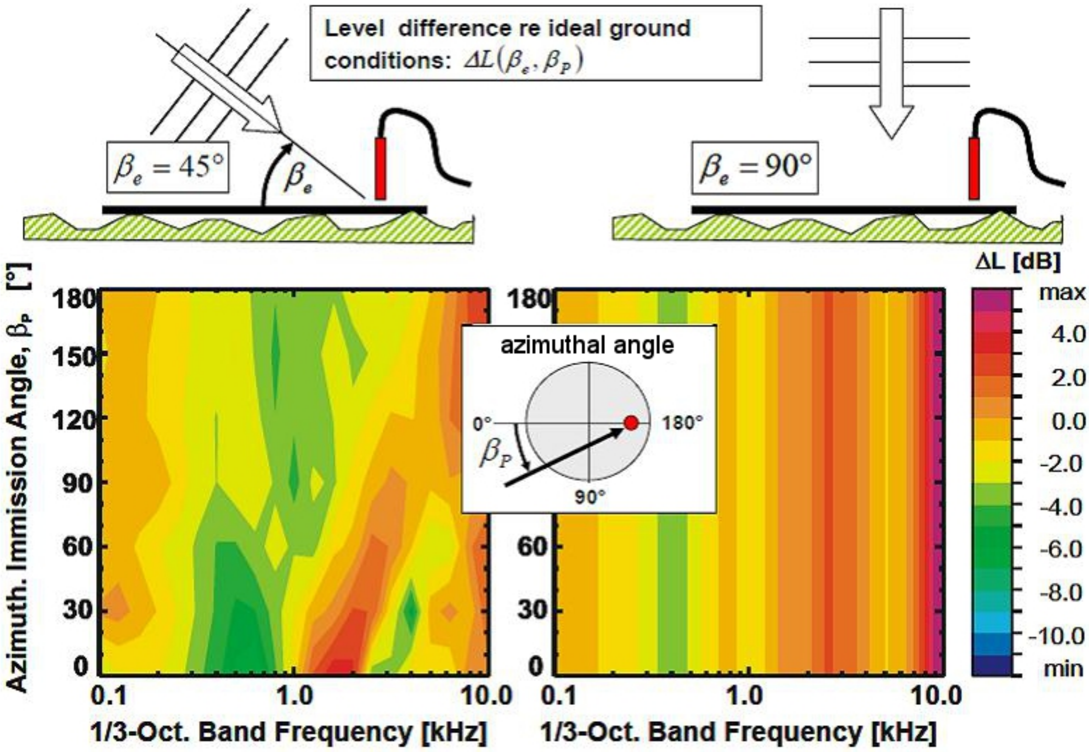

Figure 5: Directivity of a microphone on a ground plate [22]. Left: sound waves coming in from the side at an angle of $\beta_e = 45°$; right: sound from directly above the plate.

In order to avoid such disturbances, the microphones should best be mounted on a large flat and acoustically hard surface, e.g. on concrete or tarmac. However, acoustic measurements often have to be set up on grassy surfaces, where microphones mounted on individual plates have to be used. The standard method is to use circular ground plates with the microphones mounted off-center in order to avoid geometric similarities for sound refraction at the edges. These plates were originally designed to measure sound from the vertical direction in investigations of general aviation aircraft. They work fine in this context. However, they have a pronounced directivity in the azimuthal direction for sound waves that reach the plate at lower polar angles. Figure 5 from the paper of Pott-Pollenske et al.[22] illustrates this effect, which can distort the measured sound pressure level by as much as ± 5 dB. The lesson to be learned from this is to avoid placing microphones near interfaces with impedance changes or at positions where they can be reached by reflected sound waves.

2.4 Data acquisition

Great care must be taken to ensure good data quality and a consistent data set that contains all the parameters that are needed for the analysis. During the flight test, the data from all microphones in the array has to be recorded simultaneously. The trajectory of the aircraft must be recorded and there must be some means of synchronising the microphone data record with the trajectory for the data analysis. A time code signal must be recorded together with the microphone data for later synchronization with the trajectory of the aircraft, which can best be monitored by recording DGPS data on the aircraft. As a backup, DLR uses an array of six laser distance meters, which is set up around the array (see figure 2). The distance meters use very low power infrared lasers. They trigger when any part of the aircraft passes the beam. From this data, it is possible to calculate the flyover altitude, the velocity over ground, and the rate of descent. NLR has used a similar method to calculate the trajectory with an array of optical sensors that trigger when an aircraft passes their line of sight [25].

The flight trajectory can be linearized to

$$\bar{x}(t) = \bar{x}_0 + \bar{u}t \tag{2}$$

where $\bar{x}_0$ is the position of the aircraft at a reference time t_0 and $\bar{u}$ its velocity vector.

3 DATA ANALYSIS

The data reduction for moving sources is performed by first compensating the Doppler frequency shift from the raw data and then applying the standard beamforming to short time segments of the data. Typically, the time segments are chosen such that the change in the emission angle is within between $\Delta\theta \leq \pm 5°$ and $10°$ of the angle of interest.

The Doppler compensation is performed by re-sampling the data at intervals determined from the local Doppler factor. In order to limit the amplitude losses from the numeric re-sampling, the sampling frequency at the data acquisition should be at least four times the maximum frequency of the analysis. The actual frequency f at the microphones must be used for this correction and not the source frequency f_e (compare equation 3) The results are rescaled to standard atmospheric conditions using the method prescribed in [12] and to a reference flight path, e.g. a rate of descent of $3°$ and an altitude of 150 m for a landing approach.

The result of the data processing are sound source maps for all one-third-octave bands within the frequency range the array was designed for. Typically, maps are calculated for the three different emission angles $\theta = 60°$ when the aircraft approaches the array, $90°$ when the aircraft is overhead, and $120°$ when the aircraft is seen from behind.

3.1 Compensating the Doppler frequency shift

The first step in analysing phased array measurements of moving sources is to compensate the Doppler frequency shift from the microphone data.

The frequency received at the microphone depends on the frequency of the source f_e and the Doppler factor:

$$f = f_e D_f \,. \tag{3}$$

The Doppler factor is a function of the flight Mach number and the emission angle relative to the flight direction:

$$D_f = \frac{1}{1 - M_f \cos\theta_e}\,. \tag{4}$$

In the time domain, the compensation of the Doppler effect consists of the interpolation of the sound pressure value at emission time from the sampled values of the time series measured at the microphone position.

The time series of the pressure signal at the source can be restored from the data recorded at the microphone, if the position of the source is known. For a moving source, this means that its trajectory has to be known as a function of time.

The time series of the microphone signal is sampled at evenly distributed time intervals with the sampling frequency f_s of the data acquisition system. Each sample received at time t has been emitted by the source at some earlier moment in time t_e:

$$t = t_e + \tau(t_e)\,. \tag{5}$$

By the time t, the sound wave has traveled through the atmosphere for the propagation time

$$\tau = r(t_e)/c\,, \tag{6}$$

which is a function of the distance r between the source and the microphone and the speed of sound c. Because the source is moving, r is a function of time. When the trajectory of the source is known, the distance $r(t_e)$ between the microphone position $\bar{x}_i$ and the source $\bar{x}_e(t_e)$ can be calculated in emission time:

$$r(t_e) = \sqrt{(x_e(t_e) - x_i)^2 + (y_e(t_e) - y_i)^2 + (z_e(t_e) - z_i)^2}\,. \tag{7}$$

Using equations 5, 6, and 7, the reception times at the microphone positions can be calculated for desired positions of the source.

Assuming an acoustic monopole source and ideal propagation, the Doppler compensated pressure signal at the source, scaled to a reference distance, can be calculated from the recorded time series:

$$p_d(t_e) = p(t_e + \tau(t_e))\; r(t_e)/r_{\mathrm{ref}}\,. \tag{8}$$

The problem is that $p(t)$ is only available at discretely sampled points along the time axis. The value of the sound pressure $p_d(t_e)$ at emission time has to be interpolated between the two samples in the recorded time series $p(t)$ before and after the time $t = t_e + \tau(t_e)$. The scaling factor $r(t_e)/r_{\mathrm{ref}}$ compensates the amplitude loss by the spherical spreading of the sound wave from the source, which is proportional to $1/r^2$. A good choice for r_{ref} is either 1 m or a reference fly-over altitude.

The compensation of the Doppler effect can be interpreted as a re-ordering of the samples of the recorded time series to their individual emission times with a subsequent re-sampling of the time series at emission time, like it is shown in figure 6: The original time series has been sampled at a frequency of f_s and consists of discrete data at time intervals of $1/f_s$ (see on the left-hand side of figure 6). From the trajectory $\bar{x}_e(t_e)$, the distance between the source and the microphone can be calculated according to equation 8 and the time series recorded at

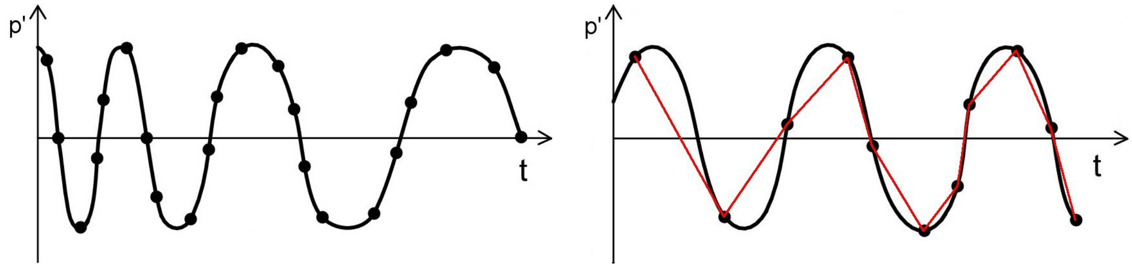

Figure 6: Compensation of the Doppler frequency shift at the microphone position by restoring the signal at the source at emission time t_e; left: Doppler-shifted time series received at the microphone, sampled at constant time intervals; right: same time series re-ordered according to the emission time, re-sampling at constant time intervals will be on the basis of the original samples (black dots connected by the red line), not the original signal (black curve).

the microphone at time t can be re-ordered into the time at which each sample was emitted at the source (see the right hand side of figure 6). For the following analysis, the calculation of frequency spectra with fast Fourier transforms or a sum-and-delay beamforming, the time series has to be available at regularly spaced time intervals with a new re-sampling frequency by interpolating the time-shifted data series.

Re-sampling causes a loss of information, especially when the time series are linearly interpolated. There is a loss of amplitude, which rises progressively with increasing frequency. For a sine wave, the amplitude loss depends on the ratio of the frequency and the sampling frequency [9, 19]. The amplitude losses in dB can be as high as

$$\Delta\mathrm{SPL} > 20\log_{10}(\cos(\pi\frac{f}{f_s}))\,. \tag{9}$$

Therefore, the sampling frequency should be as high as possible, at least four times the maximum frequency to be analysed. Of course, this error can be reduced with better interpolation methods.

For emission angles in the forward arc, the observed frequency is Doppler shifted upwards, in the rear arc, the observed frequency is lower than the frequency of the source. This means that the time series from the rear arc is better sampled than that in the forward arc.

3.2 Beamforming analysis for moving sources

The microphone data acquired during a fly-over test have to be analysed using the classical beamforming algorithm in the time domain [13], because the frequencies of the sources change with the movement of the source relative to the microphones.

While sidelobe patters in beamforming for stationary conditions stay in one frequency band, the side lobe pattern for moving sources is spread over a wide frequency range. Figure 7 presents the point-spread-functions of a linear microphone array for a stationary source and a moving source. The beamforming algorithm correctly estimates the source at the position $x = 0$, and

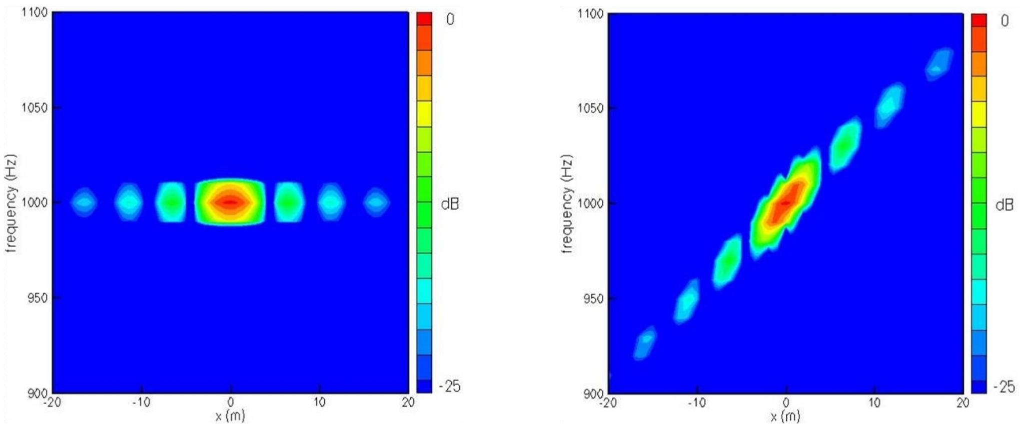

Figure 7: Point spread function of a linear microphone array as a function of the distance x parallel to the array and the frequency f; for a stationary source (left) and for a moving source (right).

generates a pattern of side lobes. In the stationary case, the side lobes stay within one frequency band (apart from a little spill-over into neighboring bands that are a side effect of the window function applied for the Fourier transform). In the case of the moving source, the side lobe pattern rotates about the centre point and shifts the side lobes into different frequency bands.

These considerations apply likewise to two-dimensional arrays. Therefore, beamforming results for moving sources have to be interpreted very carefully, because side lobes of sound sources may appear at different locations in different frequency bands.

3.3 Examples

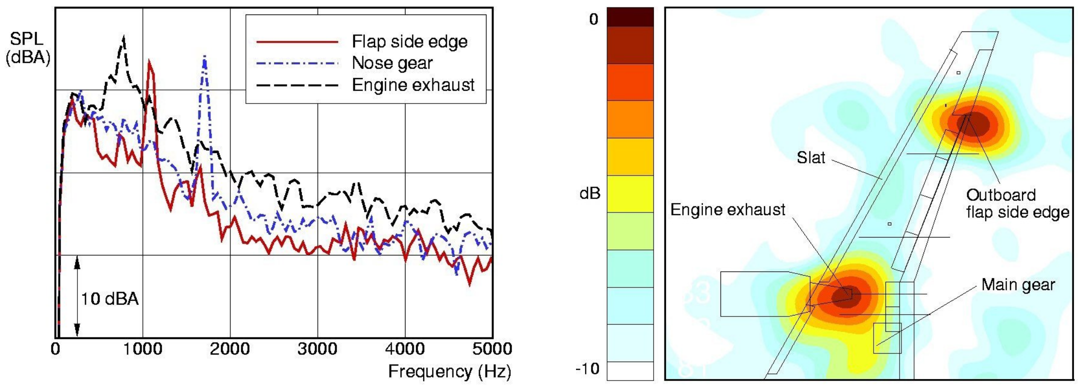

Figure 8: Sound sources on the wing of the A319; left: spectra from the beamforming analysis focused on the flap-side-edge, the nose gear, and the engine exhaust; right: a source map of the A319 wing in the 1 kHz one-third-octave-band (DLR data, analysed in cooperation with RWTH Aachen).

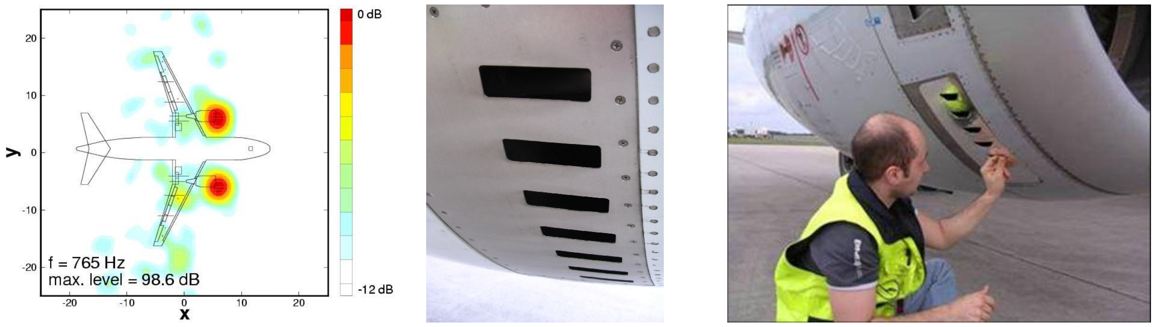

Figure 9: Modification of the de-icing system vent openings in the nacelle of the CFM56-5A engine that suppresses an 800 Hz tone; left: source map, centre: original vents, right: geometric modification.

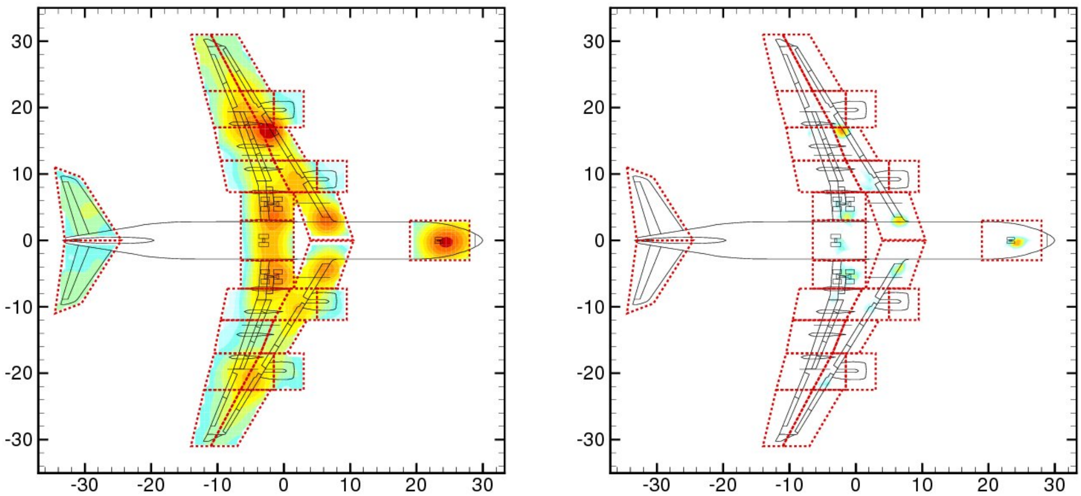

Figure 10: Source maps of an A340 in the 4 kHz one-third-octave band with a dynamic range of 15 dB; left: classical beamforming, rigth: deconvolution method.

The beamforming analysis can provide source maps and also frequency spectra for specific source points. Figure 8 shows focused spectra for the flap-side-edge, the nose gear and the engine exhaust regions of the wing of the A319 together with a source map of the wing in the 1 kHz one-third-octave band, with the sources at the engine exhaust and at the flap-side-edge. Another example are the two tones at 523 Hz and 578 Hz which make up the acoustic signature of the A319 during approach before the high-lift devices are deployed. During the 2001 array measurements performed by DLR and Lufthansa, the over-pressure valve openings of the fuel tanks under the wings were identified as the sources of these tones and a simple ramp-shaped device was developed by DLR that suppresses them [5]. A vortex generator designed by DLR was also found to suppress the tones.

Figure 12 presents the analysis of a tonal source on the MD-11 aircraft in the clean airframe configuration. The tone of 790 Hz is generated at two openings of the drain-mast under the

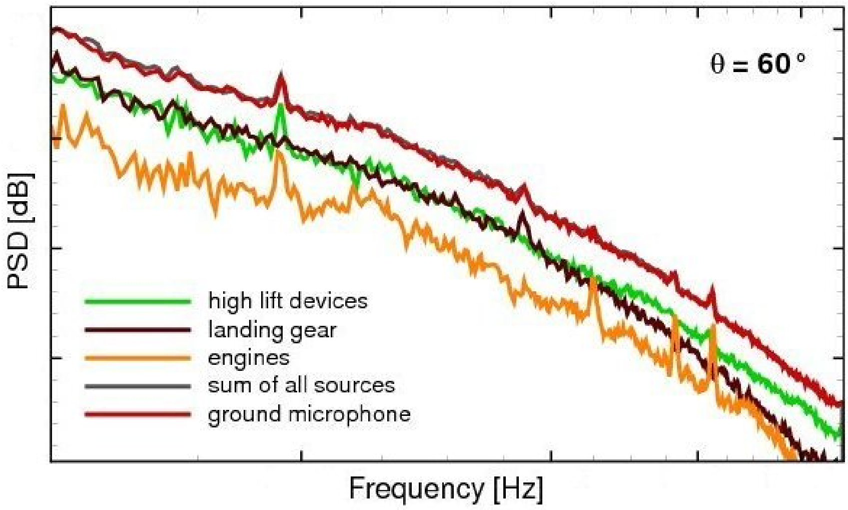

Figure 11: frequency spectra from the deconvolution analysis of the flyover in figure 10 for the reference microphone on the ground and for the integrated source regions at the high-lift devices, the landing gear and the engines.

fuselage of the MD-11.

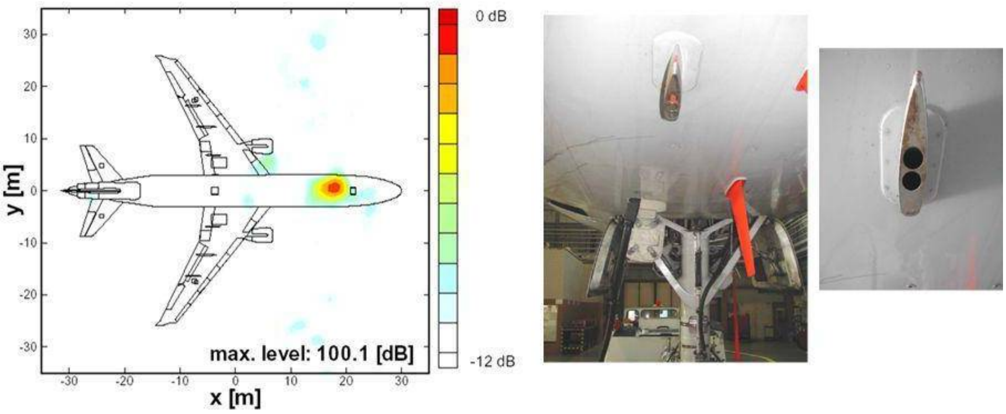

Figure 12: Cavity noise generated at the drain mast of the MD-11: left: sound source map in the 790 Hz one-third-octave band at $\theta = 90°$; center: view under the fuselage downstream of the nose landing gear; right: the drain mast with its two cavities

Sometimes a sound source can be localized, but it is not so easy to identify how it is produced. A319 aircraft with CFM56-5A engines emit a tone at about 800 Hz, which could be localized in the region to the right of the engine inlet. After extensive investigations, including acoustic measurements of the engine in a static test bed with different modifications, the sources were identified as the ventilation openings of the de-icing system on the right-hand side of the nacelles and a noise canceling modification was developed and tested by DLR and Lufthansa

Technik [5] (see figure 9).

The classical beamforming serves well to determine sound source maps and frequency spectra for specific points of the aircraft. However, because of the nonlinear imaging properties of the microphone array, the classical beamforming approach does not yield correct quantitative results. The sound source maps emphasize point sources, but it is difficult to estimate the source levels of extended sources like the slat or flap regions of aircraft wings.

3.4 Deconvolution analysis for moving sources

Guerin et al. [7] have extended the deconvolution approach for the mapping of acoustic sources (DAMAS), that had been developed by [3] and [4], to the analysis of moving sources.

The underlying idea is that the imaging properties of the microphone array can be compensated in the data analysis. For moving sources, the added difficulty is that the point spread function is not a function of space alone, but that it also varies with the frequency because of the Doppler Effect (see figure 7). As a consequence, aliases and side-lobes of one source show at different positions in different frequency bands.

The method described in [7] takes a hybrid approach to the problem: the beamforming is performed in the time domain while the point spread functions are approximated in the frequency domain.

Figure 10 illustrates the improvement of both the spatial resolution and the dynamic range obtained from the deconvolution method in comparison with the classical beamforming. It shows the source maps of an A340 at $\theta = 90^\circ$ in the 4 kHz band obtained from the classical beamforming and from the deconvolution method. The integration zones for different source regions are indicated in the figure for the landing gears, the engine inlet and exhaust, the leading and the trailing edges of the wings.

An integration of the sound pressure levels over the source regions yields quantitative results for these sources. They can be used to compare and rank the contributions of each device to the total noise emitted by the aircraft. Figure 11 presents a comparison of the spectrum measured with a single reference microphone on the ground with the spectra obtained from the integration zones for the different devices. The integrated sound pressure level from the source regions of the engines, the high-lift devices and the landing gear accounts for almost all the energy contained in the reference spectrum from the ground microphone.

The deconvolution method improves the spatial resolution and the dynamic range of the source maps and allows a quantitative analysis. The amplitudes of the sound sources can be integrated over different source regions on the aircraft. This way, it is possible to compare distributed and point sources on a quantitative basis. From the frequency spectra of individual source regions, ranking tables can be compiled and compared for different flight configurations. These tables can be used to determine critical areas, where design changes or add-on devices can be used most effectively in order to reduce the overall sound emission of the aircraft.

4 CONCLUSIONS

Fly-over measurements with phased microphone arrays have become a standard method to analyse sound sources of aicraft. The method has been developed by research institutions and industry and has now reached a level of maturity where aircraft manufacturers like Airbus, Boeing, and Embraer use it during their development cycle and for trouble shooting. The way the method is employed differs in the software used and the way the microphone arrays are set up. Usually, a compromise has to be found between the demand for good spatial and dynamic resolution and the restrictions imposed by the exerimental conditions. There is a need for simple array arrangements that are easily set-up while still providing good acoustic boundary conditions. The best place to set up a microphone array is the acoustically hard surface of an airport runway or a sufficiently large hard ground plate. Small microphone plates or microphones mounted above ground compromise the acoustic results because of wave refraction and interference. The analysis of the array data with deconvolution methods allows a quantitative analysis and a ranking of the sources.

References

[1] B. Barsikow, W. F. King III, and E. Pfizenmaier. "Wheel/rail noise generated by a high-speed train investigated with a line array of microphones." *J. Sound Vib.*, 118, 99–122, 1987.

[2] J. Billingsley and R. Kinns. "The acoustic telescope." *J. Sound Vib.*, 48, 485–510, 1976.

[3] T. Brooks and W. Humphreys. "A deconvolution approach for the mapping of acoustic sources (DAMAS) determined from phased microphone arrays." In *10th AIAA/CEAS-Aeroacoustics Conference, Manchester*. 2004. AIAA Paper 2004-2954.

[4] R. Dougherty. "Extensions of DAMAS and benefits and limitations of deconvolution in beamforming." In *11th AIAA/CEAS-Aeroacoustics Conference, Monterey*. 2005. AIAA Paper 2005-2961.

[5] R. Ewert, M. Pott-Pollenske, H. Siller, and R. König. "Forschungsverbund Leiser Verkehr, Bereich 5000 - Leises Verkehrsflugzeug, Verbundprojekt FREQUENZ, Schlussbericht, http://edok01.tib.uni-hannover.de/edoks/e01fb09/60399122xl.pdf." Technical report, DLR, 2009.

[6] S. Guérin, U. Michel, H. Siller, U. Finke, and G. Saueressig. "Airbus A319 database from dedicated flyover measurements to investigate noise abatement procedures." In *12th AIAA/CEAS-Aeroacoustics Conference, Monterey, California, USA*. 2005. AIAA Paper 2005-2981.
URL `http://elib.dlr.de/21117`

[7] S. Guérin and H. Siller. "A hybrid time-frequency approach for the noise localization analysis of aircraft fly-overs." In *14th CEAS/AIAA Aeroacoustics Conference*. 2008. ISBN 978-1-56347-939-7. AIAA Paper 2008-2955.
URL `http://elib.dlr.de/57813`

[8] S. Guérin, C. Weckmüller, and U. Michel. "Beamforming and deconvolution for aerodynamic sound sources in motion." BeBeC-2008-16, 2006. Proceedings on CD of the 1st Berlin Beamforming Conference, 22–23 November, 2006.
URL `http://www.bebec.eu/Downloads/BeBeC2006/Papers/BeBeC-2006-16_Guerin_Weckmueller_Michel.pdf`

[9] G. P. Howell, M. A. Bradley, M. A. McCormick, and J. D. Brown. "De-Dopplerization and acoustic imaging of aircraft Flyover noise measurements." *J. Sound Vib.*, 105(1), 151–167, 1986. doi:10.1016/0022-460X(86)90227-0.

[10] ICAO. "ANNEX 16 to the Convention on International Civil Aviation, Environmental Protection. Volume I - Aircraft Noise. 5th edition, incorporating Amendments 1-9." Technical report, ICAO, 2008. 228 pages.

[11] ISO 3891. "Acoustics – Procedure for Describing Aircraft Noise Heard on the Ground." International Standard, International Organisation for Standardization, 1978.

[12] ISO 9613-1. *Acoustics: Attenuation of sound during propagation outdoors*. International Organisation for Standardisation (ISO), Geneva, Switzerland, 1993.

[13] D. H. Johnson and D. E. Dudgeon. *Array Signal Processing, Concepts and Techniques*. P T R Prentice Hall, Englewood Cliffs, 1993.

[14] U. Michel, B. Barsikow, and B. Haverich. "Investigation of airframe and jet noise in high-speed flight with a microphone array." In *3rd AIAA/CEAS Aeroacoustics Conference, Atlanta*. 1997. AIAA paper 1997-1596.

[15] U. Michel, B. Barsikow, B. Haverich, and M. Schüttpelz. "Investigation of airframe and jet noise in high-speed flight with a microphone array." AIAA-1997-1596, 1997. 3rd AIAA/CEAS Aeroacoustics Conference, Atlanta, Ga, May 12-14, 1997. URL `http://bebec.eu/Downloads/Beamforming_Repository/AIAA-1997-1596_Michel_etal.pdf`

[16] U. Michel, B. Barsikow, J. Helbig, M. Hellmig, and M. Schüttpelz. "Flyover noise measurements on landing aircraft with a microphone array." AIAA Paper 98-2336, 1998. 4th AIAA/CEAS Aeroacoustics Conference, Toulouse, France, June 2-4, 1998.

[17] W. Neise. "Lärmoptimierte An- und Abflugverfahren (LAnAb): zusammenfassender Schlussbericht; Forschungsverbund "Leiser Verkehr", Bereich "Leises Verkehrsflugzeug", Projekt 1600 lärmoptimierte An- und Abflugverfahren (LAnAb)." Technical report, DLR intitute of propulsion research, engine acoustics, 2007. Http://edok01.tib.uni-hannover.de/edoks/e01fb08/565894943.pdf.

[18] J. Piet, R. Davy, G. Elias, H. Siller, L. Chow, C. Seror, and F. Laporte. "Flight test investigation of add-on treatments to reduce aircraft airframe noise." In *11th AIAA/CEAS Conference, Monterey, CA (USA)*. 2005. AIAA Paper 2005-3007. URL `http://elib.dlr.de/21168`

[19] J.-F. Piet, U. Michel, and P. Böhning. "Localization of the acoustic sources of the a340 with a large phased microphone array during flight tests." In *8th AIAA/CEAS Aeroacoustics Conference, Breckenridge, Colorado, USA*. 2002. AIAA paper 2002-2506. URL `http://elib.dlr.de/757`

[20] J.-F. Piet and G. Élias. "Airframe noise source localization using a microphone array." AIAA-1997-1643, 1997. 3rd AIAA/CEAS Aeroacoustics Conference, Atlanta, Ga, May 12-14, 1997.
URL `http://pdf.aiaa.org/preview/1997/PV1997_1643.pdf`

[21] J.-F. Piet, G. Élias, and P. Lebigot. "Localization of acoustic source from a landing aircraft with a microphone array." AIAA-1999-1811, 1999. 5th AIAA/CEAS Aeroacoustics Conference, Bellevue, Washington, USA, May 10-12, 1999.
URL `http://pdf.aiaa.org/preview/1999/PV1999_1811.pdf`

[22] M. Pott-Pollenske, W. Dobrzynski, H. Buchholz, S. Guérin, G. Saueressig, and U. Finke. "Airframe noise charakteristiks from flyover measurements and predictions." In *12th AIAA/CEAS Aeroacoustics Conference, Cambridge, Massachusetts*. 2006. AIAA paper 2006-2567.

[23] G. Saueressig, W. Dobrzynski, S. Guérin, S. Fröhlich, J. Jaegle, B. Kiefner, M. Kutner, U. Michel, M. Pott-Pollenske, H. Siller, A. Uhl, and K. Haag. "Frequenz part 3 - investigation of noise reducing retrofit measures for existing aircraft." In *EURONOISE 2006*. 2006. 2006-05-30 - 2006-06-01;.
URL `http://elib.dlr.de/47076`

[24] P. Sijtsma and R. Stoker. "Determination of Absolute Contributions of Aircraft Noise Components Using Fly-over Array Measurements." AIAA-2004-2958, 2004. 10th AIAA/CEAS Aeroacoustics Conference, Manchester, United Kingdom, 10-12 May 2004.

[25] P. Sijtsma and H. van der Waal. "Identification of noise sources on civil aircraft in approach using a phased array of microphones." Technical Report NLR-TP-2004-166, NLR, 2004.

[26] H. Siller and U. Michel. "Buzz-saw noise spectra and directivity from flyover tests." In *8th AIAA/CEAS Aeroacoustics Conference, Breckenridge, Colorado, USA*. 2002. AIAA Paper no. AIAA-2002-2562.
URL `http://elib.dlr.de/761`

[27] H. Siller, U. Michel, C. Zwiener, and G. Saueressig. "Reduction of approach noise of the md-11." In *12th AIAA/CEAS-Aeroacoustics Conference, Cambridge, Massachusets*. 2006. AIAA paper 2006-2464.
URL `http://elib.dlr.de/851`

[28] R. Stoker and Y. Guo. "Airframe Noise Source Locations of a 777 Aircraft in Flight and Comparison with Past Model-Scale Tests." AIAA-2004-3232, 2004. 10th AIAA/CEAS Aeroacoustics Conference, Manchester, United Kingdom, 10-12 May 2004.

[29] R. W. Stoker, Y. Guo, C. Streett, and N. Burnside. "Airframe Noise Source Locations of a 777 Aircraft in Flight and Comparisons with Past Model-Scale Tests." AIAA-2003-3232, 2003. 9th AIAA/CEAS Aeroacoustics Conference and Exhibit, Hilton Head, South Carolina, May 12-14, 2003.